On the geometry of demixing: A study of lipid phase separation on curved surfaces

Rinaldin, M.

Appendix

No.	Name	Sequence
1	10 nm Base	Cholesterol-TEG-3′-GTT-AGC-CCG-ATT-ACA-GAG-CGT--TCT-TT-3′
2	10 nm Inert	Cholesterol-TEG-5′-TTT-GAA-CGC-TCT-GTA-ATC-GGG--CTA-AC-3′
3	20 nm Base	Cholesterol-TEG-3′-TTT-TAG-CGA-TGG-GAA-GCG-TGT--CAG-TTA-GAT-CTC-TCG-GGA-CGG-AAT-GC-5′
4	20 nm Inert	Cholesterol-TEG-5′-TTT-ATC-GCT-ACC-CTT-CGC-ACA--GTC-AAT-CTA-GAG-AGC-CCT-GCC-TTA-CGA- 3′
5	20 nm Single Linker A	Cholesterol-TEG-5′-TTT-ATC-GCT-ACC-CTT-CGC-ACA--GTC-AAT-CTA-GAG-AGC-CCT-GCC-TTA-CGA-*GTA-GAA*--*GTA-GG*-3′-6FAM
6	20 nm Single Linker A′	Cholesterol-TEG-5′-TTT-ATC-GCT-ACC-CTT-CGC-ACA--GTC-AAT-CTA-GAG-AGC-CCT-GCC-TTA-CGA-*CCT-ACT*--*TCT-AC*-3′-Cy3
7	30 nm Base	5′-TCG-TAA-GGC-AGG-GCT-CTC-TAG-ACA-GGG-CTC-TCT--GAA-TGT-GAC-TGT-GCG-AAG-GTG-ACT-GTG-CGA-AGG--GTA-GCG-ATT-TT-3′
8	30 nm Single Linker A	Double Stearyl-HEG-5′-TT-TAT-CGC-TAC-CCT-TCG--CAC-AGT-CAC-CTT-CGC-ACA-GTC-ACA-TTC-AGA-GAG--CCC-TGT-CTA-GAG-AGC-CCT-GCC-TTA-CGA-*GTA-GAA*--*GTA-GG*-3′-6FAM
9	30 nm Single Linker A′	Double Stearyl-HEG-5′-TT-TAT-CGC-TAC-CCT-TCG--CAC-AGT-CAC-CTT-CGC-ACA-GTC-ACA-TTC-AGA-GAG--CCC-TGT-CTA-GAG-AGC-CCT-GCC-TTA-CGA-*CCT-ACT*--*TCT-AC*-3′-Cy3

Table A.1: Summary of all DNA strand sequences and their names. Sticky ends are marked in cursive.

Sphere	**Cube**	**Symm. dumbbell**	**Asymm. dumbbell**
18 ± 3	11 ± 1	13 ± 1	13 ± 2
26 ± 2	22 ± 2	23 ± 5	32 ± 2
35 ± 3	28 ± 3	50 ± 2	
45 ± 3	$41 \pm 2.$	57 ± 4	
52 ± 5	52 ± 2	67 ± 2	
58 ± 2	60 ± 2	80 ± 2	
69 ± 2	72 ± 2	89 ± 1	
80 ± 8	80 ± 1		

Table A.2: Area fractions in percentage of liquid disordered phase of the CSLBs shown in Chapter 3, Figure 3.6.

BSM [%]	POPC [%]	chol [%]
30	50	20
35	45	20
40	35	25
50	20	30
50	25	25

Table A.3: Lipid mixtures allowing for phase separation.

Lipid composition. In supported lipid bilayers, the substrate can affect the physical properties of phase separation, such as the temperature at which phase separation occurs [71]. Therefore, we varied the lipid composition on spherical supports to identify the conditions under which phase separation occurs. We found that phase separation can be obtained with mixtures of porcine brain sphingomyelin (BSM), 1-palmitoyl-2-oleoyl-sn-glycero-3-phosphocholine(POPC) and cholesterol (chol) in mole ratios equal to the ones reported on Table A.3.
No phase separation was observed for 0 to 10% of cholesterol on spherical CSLBs. We used the mixture 2:1:1 BSM:POPC:chol. This ratio has also been shown to phase separate in free-standing bilayers both at 23°C and 37°C, albeit with a different type of sphingomyelin, the palmitoylsphingomyelin PSM [140]. We confirmed that for our mixture phase separation also occurs in free standing bilayers (giant unilamellar vesicles) made via electro-swelling (see Figure A.1).

Surface properties analysis. To exclude that surface properties of the supporting colloidal particles, such as the roughness or the type of silica, affect the phase separation landscape, we compared dumbbell shaped CSLBs made on two different types of dumbbell-shaped substrates: silica dumbbells made via destabilisation of colloidal silica spheres and silica-coated dumbbells made from PS-TPM-Si particles particles. We studied the likelihood of phase separation and of number of domains. We observed that these quantities are similar

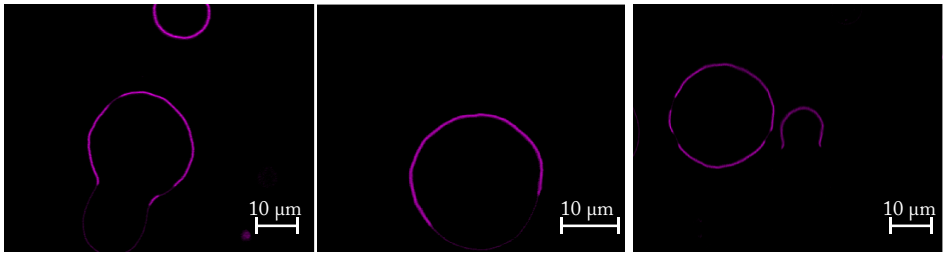

Figure A.1: Fluorescence images of phase-separated giant unilamellar vesicles. Lipid composition 2:1:1 of SM:POPC:chol. The liquid disordered phase is labelled in magenta with DOPE-Rhodamine.

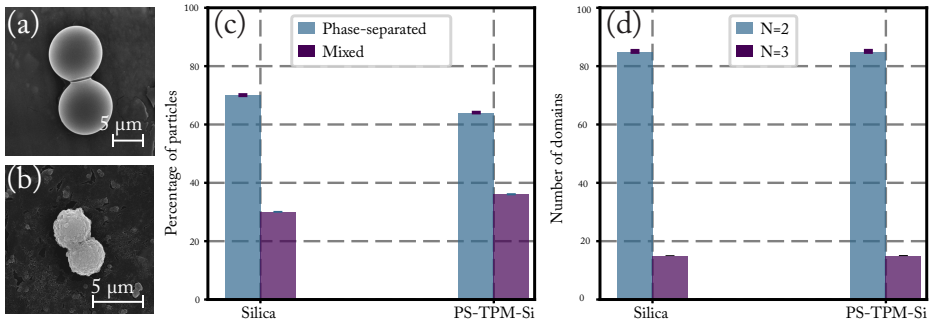

Figure A.2: Analysis of the surface effect. (a) Scanning electron microscopy (SEM) image of a silica dumbbell made via destabilisation of silica spheres. **(b**) SEM image of a PS-TPM-Si dumbbell. **(c)** Percentage of phase separation of dumbbell shaped CSLBs made of aggregated silica spheres (left) and PS-TPM-Si dumbbells (right). **(d)** Percentage of number of coexistent liquid ordered and disordered domains of the same CSLBs as before.

for the two types of particles, indicating that the properties of the surfaces of the supports that we use do not significantly influence phase separation properties (Figure A.2).

Details on the numerical simulations of Chapter 3. Here, we explain how we constructed the 3D geometries corresponding to the experimental CSLBs and how we implemented the numerical solver to find equilibrium configurations relative to Equation 3.4 and 3.5, which were essential to produce Figure 3.8 and 3.9.

Gradient Flows

The general strategy to find the equilibria of phase-field models is to implement an evolution equation that flows an arbitrary configuration smoothly towards energy minima. Extending previous work[168] we choose to implement a gradient flow with conserved global order parameter:

$$\partial_t \phi = \epsilon \nabla^2 \phi - \frac{1}{\epsilon} f'(\phi) - k'(\phi) H^2 - \bar{k}'(\phi) K + \lambda \,, \tag{A.1}$$

where ∇^2 is the Laplace-Beltrami operator on S and $\phi = \phi(x^i, t)$ has been promoted to a function of both space and flow parameter t. The right hand side consists just of (minus) the first functional derivative of the total free energy with a term involving the conservation of the total concentration. When minimising Equation 3.5 one has to replace $k(\phi) \to k(\phi)/\epsilon$ and $\bar{k}(\phi) \to \bar{k}(\phi)/\epsilon$ in the dynamical equation.

The flow generated by Equation A.1 is fictitious and does not reflect the actual coarsening dynamics of the binary fluid. This approach offers nonetheless a practical way to generate stable equilibrium configurations for arbitrary geometries. Note that t has dimension of a length.

The numerical integration of Equation A.1 is done via a local Runge-Kutta-Fehlberg adaptive time-step algorithm[220], where the criterion for acceptance of a given time-step is averaged over S.

Metastable equilibrium is defined as the fixed point of the right hand side of Equation A.1, *i.e.* when $\partial_t \phi$ vanishes everywhere. Numerically, we assume that the simulation has reached equilibrium when the surface-averaged squared time-derivative

$$\left\langle (\partial_t \phi)^2 \right\rangle_S = \frac{1}{A_S} \int_S \mathrm{d}A \, (\partial_t \phi)^2 \,, \tag{A.2}$$

decreases below a given threshold (usually of the order of 10^{-6} for surfaces of unit area).

The initial conditions, at $t = 0$, are either random ϕ values distributed around a specific Φ value (for Equation 3.5) or a random set of small domains with constant $\phi = \phi_*$ surrounded by a $1 - \phi_*$ background (for Equation 3.4 and to generate the phase diagram of Figure 3.8a).

Mesh construction

We solve Equation A.1 numerically using a finite difference scheme on unstructured triangular meshes. Meshes are constructed using the software package *Gmsh*[190]. As in the case of planar droplets on the plane, the rotational symmetry of the substrate is not necessarily inherited by the minimisers of the Gibbs free energy, thus it is often necessary to solve the full two-dimensional problem. For the case of dumbbells and snowmen, the

radial profile has been obtained by joining two circular arcs by an interpolating polynomial of degree eight, chosen such that the neck interpolation and the circular arc match smoothly up to the fourth derivative at each of the two gluing points.

Due to the arbitrariness of the geometry of S, our implementation of the solver is entirely coordinate-independent. Computation of discrete Laplace-Beltrami weights and of the mean curvature H on each node is done by using the cotangent method. Since the ideal surface is smooth and differentiable at least twice, we use the numerically computed H as a criterion for the quality of the triangulation: if H appears to be reasonably smooth on every portion of S we accept the mesh, otherwise we refine it.

For every triangulation, the length scale in a simulation is fixed by the requirement that the area of S has to match the dimensions in μm^2 of the observed CSLBs. Furthermore, the value of ϵ is automatically computed for each triangulation and is fixed by the requirement that the interface should be resolved anywhere on the membrane by at least six grid points.

Equilibrium equation in non-homogeneous potentials

If the free energy depends explicitly on the position through the non-constancy of curvatures, one can divide S in regions - each labelled by an index i - where both H and K can be regarded as approximately constant so that

$$F = \sum_i \varphi_i F_i(\phi_i)\,, \tag{A.3}$$

where the sum runs over the partition of S, φ_i is the area fraction occupied by the subregion i (so that $\sum_i x_i = 1$). The variable ϕ_i is the restriction of the field ϕ to the region i. If S is a smooth surface, it is always possible to find partitions that satisfy the above requirement to an arbitrary degree of accuracy. The condition for equilibrium is obtained by differentiating G in each subdomain:

$$\frac{\mathrm{d}F_i}{\mathrm{d}\phi_i} = \mu\,, \tag{A.4}$$

provided the average concentration

$$\sum_i \varphi_i \phi_i = \Phi\,, \tag{A.5}$$

is kept fixed. Equation A.4 implies that, at equilibrium, the derivative of each free energy has to take the same value over all of S. This should not be confused with the usual requirement that, at equilibrium, two coexisting phases always have the same value of the chemical potential: here the free energies are position-dependent functions and Equation A.4 refers to the equilibrium condition of a single, mixed phase in different locations in space. Note that now, for generic curvature dependence, the mixed phase $\phi_i = \Phi$ is not a solution of Equation A.4. If some, or all, F_i happen to be concave, then one should check whether the spinodally decomposed solutions can become locally favoured. We found the solutions of Equation A.4 when S consists of the disjoint union of two spheres to produce the equilibrium phase diagrams of Figure 3.9b-d.

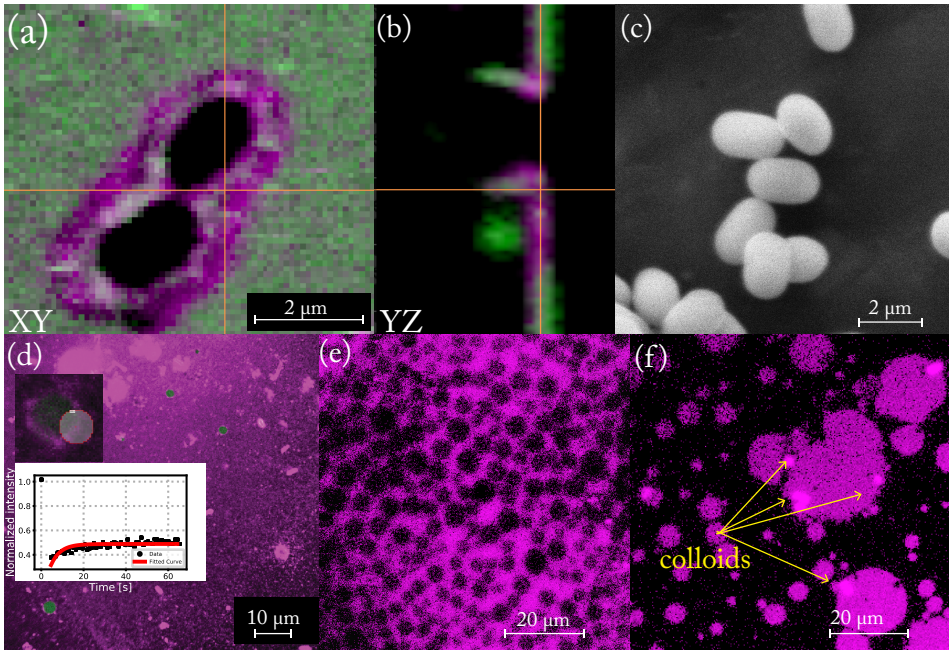

Figure A.3: Phase separation on a flat substrate. Fluorescence microscopy image of a lipid bilayer on a cluster of two colloidal sphero-cylinders silica shells obtained from a synthesis procedure analogous to the one of the colloidal cubic shells. The projections of the bilayer on the **(a)** XY and **(b)** YZ planes are reported to show the localisation of the LD phase at the contact area between the colloids and the flat substrate. **(c)** SEM image of the sphero-cylinders. **(d)** Fluorescence microscopy image of a lipid bilayer on a flat substrate without colloids taken five days after lipid coating. Circular LO domains are surrounded by LD domains. In the inset, we report the result of a FRAP experiment on the the bleached area indicated with a red circle. We can observe that the fraction of mobile lipids decreased over the five days. **(e)** Fluorescence image of a phase-separated bilayer on MICA substrate, where only the LD phase was labelled in magenta. We can observe circular domains. **(f)** Fluorescence image of a phase-separated bilayer on a MICA substrate with colloidal particles attached. The particles are indicated in yellow. By comparing the two figures, we can hypothesise that the colloids may alter the regular pattern of circular domains shown in (e).

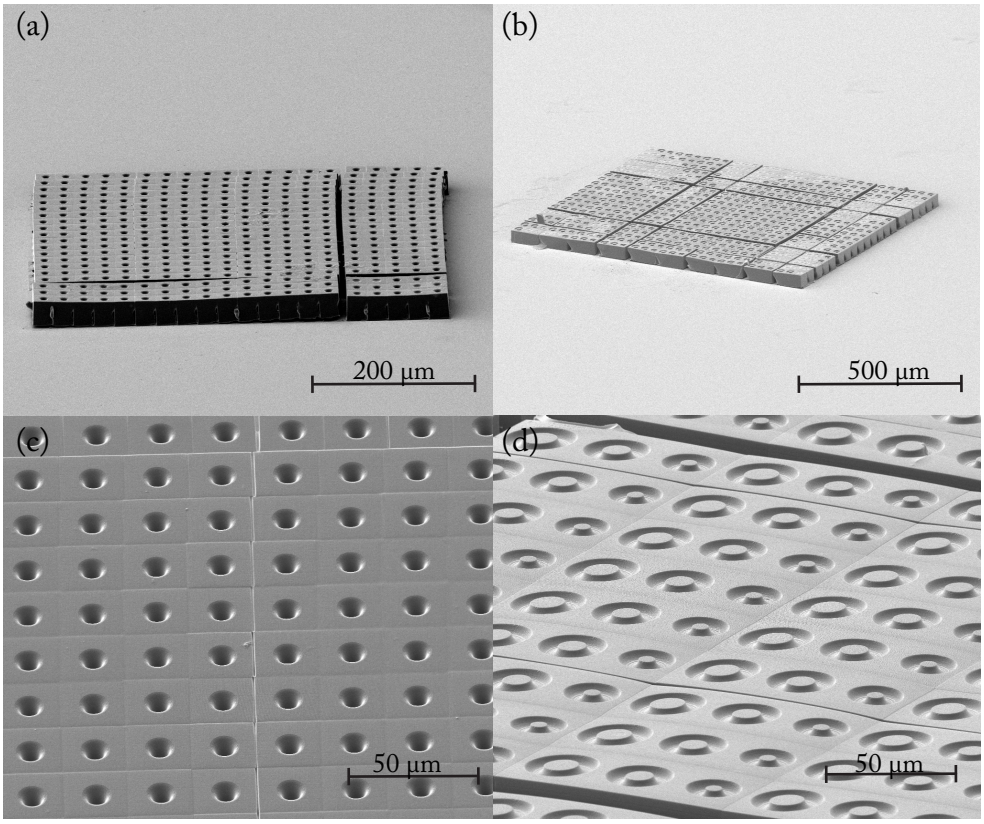

Figure A.4: SEM images of micro-printed molds. (a)-(c) Two views of molds of inverted Gaussian bumps. **(b)-(d)** Two views of molds of inverted torii.

Bibliography

[1] Alberts, B.; Johnson, A.; Lewis, J.; Morgan, D.; Raff, M.; Roberts, K.; Walter, P. Molecular Biology of the Cell, Sixth Edition. Taylor & Francis Group, **2014**.

[2] Sezgin, E.; Levental, I.; Mayor, S.; Eggeling, C. The mystery of membrane organization: composition, regulation and roles of lipid rafts. *Nat. Rev. Mol. Cell Biol.* **2017**, 18 (6), 361.

[3] Rayermann, S. P.; Rayermann, G. E.; Cornell, C. E.; Merz, A. J.; Keller, S. L. Hallmarks of Reversible Separation of Living, Unperturbed Cell Membranes into Two Liquid Phases. *Biophys. J.* **2017**, 113 (11), 2425–2432.

[4] Baumgart, T.; Hess, S. T.; Webb, W. W. Imaging coexisting fluid domains in biomembrane models coupling curvature and line tension. *Nature* **2003**, 425 (6960), 821.

[5] Subramaniam, A. B.; Lecuyer, S.; Ramamurthi, K. S.; Losick, R.; Stone, H. A. Particle/fluid interface replication as a means of producing topographically patterned polydimethylsiloxane surfaces for deposition of lipid bilayers. *Adv. Mater.* **2010**, 22 (19), 2142–2147.

[6] Roux, A.; Cuvelier, D.; Nassoy, P.; Prost, J.; Bassereau, P.; Goud, B. Role of curvature and phase transition in lipid sorting and fission of membrane tubules. *EMBO J.* **2005**, 24 (8), 1537–1545.

[7] Sorre, B.; Callan-Jones, A.; Manneville, J.-B.; Nassoy, P.; Joanny, J.-F.; Prost, J.; Goud, B.; Bassereau, P. Curvature-driven lipid sorting needs proximity to a demixing point and is aided by proteins. *Proc. Natl. Acad. Sci. U.S.A.* **2009**, 106 (14), 5622–5626.

[8] Tian, A.; Baumgart, T. Sorting of lipids and proteins in membrane curvature gradients. *Biophys. J.* **2009**, 96 (7), 2676–2688.

[9] Battisti, I.; Bastiaans, K. M.; Fedoseev, V.; De La Torre, A.; Iliopoulos, N.; Tamai, A.; Hunter, E. C.; Perry, R. S.; Zaanen, J.; Baumberger, F.; et al. Universality of pseudogap and emergent order in lightly doped Mott insulators. *Nat. Phys.* **2017**, 13 (1), 21.

[10] Nott, T. J.; Petsalaki, E.; Farber, P.; Jervis, D.; Fussner, E.; Plochowietz, A.; Craggs, T. D.; Bazett-Jones, D. P.; Pawson, T.; Forman-Kay, J. D.; et al. Phase transition

of a disordered nuage protein generates environmentally responsive membraneless organelles. *Mol. Cell* **2015**, 57 (5), 936–947.

[11] Veatch, S. L.; Keller, S. L. Separation of liquid phases in giant vesicles of ternary mixtures of phospholipids and cholesterol. *Biophys. J.* **2003**, 85 (5), 3074–3083.

[12] Semrau, S.; Schmidt, T. Membrane heterogeneity–from lipid domains to curvature effects. *Soft Matter* **2009**, 5 (17), 3174–3186.

[13] Heberle, F. A.; Feigenson, G. W. Phase separation in lipid membranes. *Cold Spring Harbor Perspect. Biol.* **2011**, 3 (4), a004630.

[14] Honerkamp-Smith, A. R.; Veatch, S. L.; Keller, S. L. An introduction to critical points for biophysicists; observations of compositional heterogeneity in lipid membranes. *Biochim. Biophys. Acta, Biomembr.* **2009**, 1788 (1), 53–63.

[15] Callan-Jones, A.; Sorre, B.; Bassereau, P. Curvature-driven lipid sorting in biomembranes. *Cold Spring Harbor Perspect. Biol.* **2011**, 3 (2), a004648.

[16] Bacia, K.; Schwille, P.; Kurzchalia, T. Sterol structure determines the separation of phases and the curvature of the liquid-ordered phase in model membranes. *Proc. Natl. Acad. Sci. U.S.A.* **2005**, 102 (9), 3272–3277.

[17] Heinrich, M.; Tian, A.; Esposito, C.; Baumgart, T. Dynamic sorting of lipids and proteins in membrane tubes with a moving phase boundary. *Proc. Natl. Acad. Sci. U.S.A* **2010**, 107 (16), 7208–7213.

[18] Parthasarathy, R.; Yu, C.-h.; Groves, J. T. Curvature-Modulated Phase Separation in Lipid Bilayer Membranes. *Langmuir* **2006**, 22 (11), 5095–5099.

[19] Feriani, L.; Cristofolini, L.; Cicuta, P. Soft pinning of liquid domains on topographical hemispherical caps. *Chem. Phys. Lipids* **2015**, 185, 78–87.

[20] Mornet, S.; Lambert, O.; Duguet, E.; Brisson, A. The Formation of Supported Lipid Bilayers on Silica Nanoparticles Revealed by Cryoelectron Microscopy. *Nano Lett.* **2005**, 5 (2), 281–285.

[21] Ryu, Y.-S.; Wittenberg, N. J.; Suh, J.-H.; Lee, S.-W.; Sohn, Y.; Oh, S.-H.; Parikh, A. N.; Lee, S.-D. Continuity of monolayer-bilayer junctions for localization of lipid raft microdomains in model membranes. *Sci. Rep.* **2016**, 6, 26823.

[22] Ryu, Y.-S.; Lee, I.-H.; Suh, J.-H.; Park, S. C.; Oh, S.; Jordan, L. R.; Wittenberg, N. J.; Oh, S.-H.; Jeon, N. L.; Lee, B.; et al. Reconstituting ring-rafts in bud-mimicking topography of model membranes. *Nat. Comm.* **2014**, 5, 4507.

[23] Miller, E. J.; Voïtchovsky, K.; Staykova, M. Substrate-led cholesterol extraction from supported lipid membranes. *Nanoscale* **2018**, 10 (34), 16332–16342.

[24] Castellana, E. T.; Cremer, P. S. Solid supported lipid bilayers: From biophysical studies to sensor design. *Surf. Sci. Rep.* **2006**, 61 (10), 429–444.

[25] Brian, A. A.; McConnell, H. M. Allogeneic stimulation of cytotoxic T cells by supported planar membranes. *Proc. Natl. Acad. Sci. U.S.A* **1984**, 81 (19), 6159.

[26] McConnell, H. M.; Watts, T. H.; Weis, R.; Brian, A. A. Supported planar membranes in studies of cell-cell recognition in the immune system. *Biochim. Biophys. Acta, Biomembr, Rev. Biomembr.* **1986**, 864 (1), 95–106.

[27] Johnson, J. M.; Ha, T.; Chu, S.; Boxer, S. G. Early steps of supported bilayer formation probed by single vesicle fluorescence assays. *Biophys. J.* **2002**, 83 (6), 3371–3379.

[28] Reimhult, E.; Höök, F.; Kasemo, B. Intact vesicle adsorption and supported biomembrane formation from vesicles in solution: influence of surface chemistry, vesicle size, temperature, and osmotic pressure. *Langmuir* **2003**, 19 (5), 1681–1691.

[29] Richter, R. P.; Bérat, R.; Brisson, A. R. Formation of solid-supported lipid bilayers: an integrated view. *Langmuir* **2006**, 22 (8), 3497–3505.

[30] Tamm, L. K.; McConnell, H. M. Supported phospholipid bilayers. *Biophys. J.* **1985**, 47 (1), 105–113.

[31] Lu, P. J.; Weitz, D. A. Colloidal particles: crystals, glasses, and gels. *Annu. Rev. Condens. Matter Phys.* **2013**, 4 (1), 217–233.

[32] Poon, W. Colloids as big atoms. *Science* **2004**, 304 (5672), 830–831.

[33] Colvin, V. L. From opals to optics: Colloidal photonic crystals. *MRS Bull.* **2001**, 26 (8), 637–641.

[34] Garg, T.; Rath, G.; Goyal, A. K. Colloidal drug delivery systems: current status and future directions. *Crit. Rev. Ther. Drug Carrier Syst.* **2015**, 32 (2).

[35] *https://www.sacannalab.com/* **2019**.

[36] Yuan, D.; Lasagni, A.; Hendricks, J. L.; Martin, D. C.; Das, S. Patterning of periodic nano-cavities on PEDOT–PSS using nanosphere-assisted near-field optical enhancement and laser interference lithography. *Nanotechnology* **2011**, 23 (1), 015304.

[37] Rossi, L.; Sacanna, S.; Irvine, W. T. M.; Chaikin, P. M.; Pine, D. J.; Philipse, A. P. Cubic crystals from cubic colloids. *Soft Matter* **2011**, 7 (9), 4139–4142.

[38] Van Blaaderen, A. Colloids under external control. *Mrs Bull.* **2004**, 29 (2), 85–90.

[39] Kraft, D. J.; Ni, R.; Smallenburg, F.; Hermes, M.; Yoon, K.; Weitz, D. A.; van Blaaderen, A.; Groenewold, J.; Dijkstra, M.; Kegel, W. K. Surface roughness directed self-assembly of patchy particles into colloidal micelles. *Proc. Natl. Acad. Sci. U.S.A.* **2012**, 109 (27), 10787–10792.

[40] Stöber, W.; Fink, A.; Bohn, E. Controlled growth of monodisperse silica spheres in the micron size range. *J. Colloid Interface Sci.* **1968**, 26 (1), 62–69.

[41] Sugimoto, T.; Sakata, K. Preparation of monodisperse pseudocubic α-Fe2O3 particles from condensed ferric hydroxide gel. *J. Colloid Interface Sci.* **1992**, 152 (2), 587–590.

[42] Cumpston, B. H.; Ananthavel, S. P.; Barlow, S.; Dyer, D. L.; Ehrlich, J. E.; Erskine, L. L.; Heikal, A. A.; Kuebler, S. M.; Lee, I.-Y. S.; McCord-Maughon, D.; et al. Two-photon polymerization initiators for three-dimensional optical data storage and microfabrication. *Nature* **1999**, 398 (6722), 51.

[43] Zhou, X.; Hou, Y.; Lin, J. A review on the processing accuracy of two-photon polymerization. *AIP Adv.* **2015**, 5 (3), 030701.

[44] Seniutinas, G.; Weber, A.; Padeste, C.; Sakellari, I.; Farsari, M.; David, C. Beyond 100 nm resolution in 3D laser lithography—Post processing solutions. *Microelectron. Eng.* **2018**, 191, 25–31.

[45] Maruo, S.; Fourkas, J. T. Recent progress in multiphoton microfabrication. *Laser Photonics Rev.* **2008**, 2 (1-2), 100–111.

[46] Wang, Y.; Wang, Y.; Breed, D. R.; Manoharan, V. N.; Feng, L.; Hollingsworth, A. D.; Weck, M.; Pine, D. J. Colloids with valence and specific directional bonding. *Nature* **2012**, 491 (7422), 51–55.

[47] Rogers, W. B.; Manoharan, V. N. Programming colloidal phase transitions with DNA strand displacement. *Science* **2015**, 347 (6222), 639–642.

[48] Wang, Y.; Wang, Y.; Zheng, X.; Ducrot, É.; Yodh, J. S.; Weck, M.; Pine, D. J.; Ducrot, E.; Yodh, J. S.; Weck, M.; Pine, D. J. Crystallization of DNA-coated colloids. *Nat. Commun.* **2015**, 6, 7253.

[49] Feng, L.; Pontani, L.-L.; Dreyfus, R.; Chaikin, P.; Brujic, J. Specificity, flexibility and valence of DNA bonds guide emulsion architecture. *Soft Matter* **2013**, 9 (41), 9816–9823.

[50] Zhang, Y.; McMullen, A.; Pontani, L. L.; He, X.; Sha, R.; Seeman, N. C.; Brujic, J.; Chaikin, P. M. Sequential self-assembly of DNA functionalized droplets. *Nat. Commun.* **2017**, 8 (1), 21.

[51] McMullen, A.; Holmes-Cerfon, M.; Sciortino, F.; Grosberg, A. Y.; Brujic, J. Freely Jointed Polymers Made of Droplets. *Phys. Rev. Lett.* **2018**, 121, 138002.

[52] Van Der Meulen, S. A.; Leunissen, M. E. Solid colloids with surface-mobile DNA linkers. *J. Am. Chem. Soc.* **2013**, 135 (40), 15129–15134.

[53] Van Der Meulen, S. A. J.; Dubacheva, G. V.; Dogterom, M.; Richter, R. P.; Leunissen, M. E. Quartz crystal microbalance with dissipation monitoring and spectroscopic ellipsometry measurements of the phospholipid bilayer anchoring stability and kinetics of hydrophobically modified DNA oligonucleotides. *Langmuir* **2014**, 30 (22), 6525–6533.

[54] Van der Meulen, S. A. J.; Helms, G.; Dogterom, M. Solid colloids with surface-mobile linkers. *J. Phys.: Condens. Matter* **2015**, 27 (23), 233101.

[55] Chakraborty, I.; Meester, V.; Van der Wel, C.; Kraft, D. J. Colloidal joints with designed motion range and tunable joint flexibility. *Nanoscale* **2017**, 9, 7814–7821.

[56] Deserno, M. Notes on Differential Geometry with special emphasis on surfaces in $\mathbb{R}^3$. *https://www.cmu.edu/biolphys/deserno/pdf/diff_geom.pdf* **2014**.

[57] Leibler, S. Curvature instability in membranes. *J. Phys.* **1986**, 47 (3), 507–516.

[58] Leibler, S.; Andelman, D. Ordered and curved meso-structures in membranes and amphiphilic films. *J. Phys.* **1987**, 48 (11), 2013–2018.

[59] Canham, P. B. The minimum energy of bending as a possible explanation of the biconcave shape of the human red blood cell. *J. Theor. Biol.* **1970**, 26 (1), 61–81.

[60] Helfrich, W. Elastic Properties of Lipid Bilayers-Theory and Possible Experiments. *Z. Naturforsch. C* **1973**, 28.

[61] Lázaro, G. R.; Pagonabarraga, I.; Hernández-Machado, A. Phase-field theories for mathematical modeling of biological membranes. *Chem. Phys. Lipids* **2015**, 185, 46–60.

[62] Seifert, U. Curvature-induced lateral phase segregation in two-component vesicles. *Phys. Rev. Lett.* **1993**, 70 (9), 1335.

[63] Jülicher, F.; Lipowsky, R. Domain-induced budding of vesicles. *Phys. Rev. Lett.* **1993**, 70 (19), 2964.

[64] Lipowsky, R. Domain-induced budding of fluid membranes. *Biophys. J.* **1993**, 64 (4), 1133–1138.

[65] Baumgart, T.; Das, S.; Webb, W.; Jenkins, J. Membrane elasticity in giant vesicles with fluid phase coexistence. *Biophys. J.* **2005**, 89 (2), 1067–1080.

[66] Semrau, S.; Idema, T.; Holtzer, L.; Schmidt, T.; Storm, C. Accurate determination of elastic parameters for multicomponent membranes. *Phys. Rev. Lett.* **2008**, 100 (8), 088101.

[67] Troutier, A. L.; Ladavière, C. An overview of lipid membrane supported by colloidal particles. *Adv. Colloid Interface Sci.* **2007**, 133 (1), 1–21.

[68] Carmona-Ribeiro, A. M. Preparation and Characterization of Biomimetic Nanoparticles for Drug Delivery. 283–294. Humana Press, Totowa, NJ, **2012**.

[69] Li, J.; Wang, X.; Zhang, T.; Wang, C.; Huang, Z.; Luo, X.; Deng, Y. A review on phospholipids and their main applications in drug delivery systems. *Asian J. Pharm. Sci.* **2015**, 10 (2), 81–98.

[70] Savarala, S.; Ahmed, S.; Ilies, M. A.; Wunder, S. L. Formation and Colloidal Stability of DMPC Supported Lipid Bilayers on SiO_2 Nanobeads. *Langmuir* **2010**, 26 (14), 12081–12088.

[71] Chemburu, S.; Fenton, K.; Lopez, G. P.; Zeineldin, R. Biomimetic silica microspheres in biosensing. *Molecules* **2010**, 15 (3), 1932–1957.

[72] Brouwer, I.; Giniatullina, A.; Laurens, N.; Weering, J. R. T. V.; Bald, D.; Wuite, G. J. L.; Groffen, A. J. Direct quantitative detection of Doc2b-induced hemifusion in optically trapped membranes. *Nat. Commun.* **2015**, 6, 8387.

[73] Sackmann, E. Supported Membranes: Scientific and Practical Applications. *Science* **1996**, 271 (5245), 43–48.

[74] Madwar, C.; Gopalakrishnan, G.; Lennox, R. B. Interfacing living cells and spherically supported bilayer lipid membranes. *Langmuir* **2015**, 31 (16), 4704–4712.

[75] Mashaghi, S.; Jadidi, T.; Koenderink, G.; Mashaghi, A. Lipid Nanotechnology. *Int. J. Mol. Sci.* **2013**, 14, 4242–4282.

[76] Kohlstedt, K. L.; Glotzer, S. C. Self-assembly and tunable mechanics of reconfigurable colloidal crystals. *Phys. Rev. E* **2013**, 87 (3).

[77] Ortiz, D.; Kohlstedt, K. L.; Nguyen, T. D.; Glotzer, S. C. Self-assembly of reconfigurable colloidal molecules. *Soft Matter* **2014**, 10 (20), 3541–3552.

[78] Smallenburg, F.; Filion, L.; Sciortino, F. Erasing no-man's land by thermodynamically stabilizing the liquid-liquid transition in tetrahedral particles. *Nat. Phys.* **2014**, 10 (9), 653–657.

[79] Hu, H.; Ruiz, P. S.; Ni, R. Entropy Stabilizes Floppy Crystals of Mobile DNA-Coated Colloids. *Phys. Rev. Lett.* **2018**, 120 (4), 048003.

[80] Joannopoulos, J. D.; Villeneuve, P. R.; Fan, S. Photonic crystals: putting a new twist on light. *Nature* **1997**, 386 (6621), 143–149.

[81] Lin, Y.; Herman, P. R.; Valdivia, C. E.; Li, J.; Kitaev, V.; Ozin, G. A. Photonic band structure of colloidal crystal self-assembled in hollow core optical fiber. *Appl. Phys. Lett.* **2005**, 86 (12), 121106.

[82] Phillips, C. L.; Jankowski, E.; Krishnatreya, B. J.; Edmond, K. V.; Sacanna, S.; Grier, D. G.; Pine, D. J.; Glotzer, S. C. Digital colloids: reconfigurable clusters as high information density elements. *Soft Matter* **2014**, 10 (38), 7468–7479.

[83] Hadorn, M.; Eggenberger Hotz, P. DNA-Mediated Self-Assembly of Artificial Vesicles. *PLoS ONE* **2010**, 5 (3), e9886.

[84] Beales, P. A.; Nam, J.; Vanderlick, T. K. Specific adhesion between DNA-functionalized Janus vesicles: size-limited clusters. *Soft Matter* **2011**, 7, 1747–1755.

[85] Parolini, L.; Mognetti, B. M.; Kotar, J.; Eiser, E.; Cicuta, P.; Di Michele, L. Volume and porosity thermal regulation in lipid mesophases by coupling mobile ligands to soft membranes. *Nat. Commun.* **2015**, 6, 5948.

[86] Milam, V. T. Oligonucleotide-based recognition in colloidal systems - opportunities and challenges. *Curr. Opin. Colloid & In. Sci.* **2016**, 26, 75–83.

[87] Schade, N. B.; Holmes-Cerfon, M. C.; Chen, E. R.; Aronzon, D.; Collins, J. W.; Fan, J. A.; Capasso, F.; Manoharan, V. N. Tetrahedral Colloidal Clusters from Random Parking of Bidisperse Spheres. *Phys. Rev. Lett.* **2013**, 110 (14), 148303.

[88] Meester, V.; Kraft, D. J. Spherical, Dimpled, and Crumpled Hybrid Colloids with Tunable Surface Morphology. *Langmuir* **2016**, 32 (41), 10668–10677.

[89] Van der Wel, C.; Bhan, R. K.; Verweij, R. W.; Frijters, H. C.; Gong, Z.; Hollingsworth, A. D.; Sacanna, S.; Kraft, D. J. Preparation of Colloidal Organosilica Spheres through Spontaneous Emulsification. *Langmuir* **2017**, 33 (33), 8174–8180.

[90] Doherty, R. P.; Kraft, D. J. One-pot surfactant-free synthesis of organosilica colloids with various surface functional groups. In preparation.

[91] Appel, J.; Akerboom, S.; Fokkink, R. G.; Sprakel, J. Facile One-Step Synthesis of Monodisperse Micron-Sized Latex Particles with Highly Carboxylated Surfaces. *Macromol. Rapid Commun.* **2013**, 34 (16), 1284–1288.

[92] Cremer, P. S.; Boxer, S. G. Formation and Spreading of Lipid Bilayers on Planar Glass Supports. *J. Phys. Chem. B* **1999**, 103 (13), 2554–2559.

[93] Antipina, A. Y.; Gurtovenko, A. A. Molecular-level insight into the interactions of DNA with phospholipid bilayers: barriers and triggers. *RSC Adv.* **2016**, 6, 36425–36432.

[94] Van der Wel, C.; Vahid, A.; Saric, A.; Idema, T.; Heinrich, D.; Kraft, D. J. Lipid membrane-mediated attraction between curvature inducing objects. *Sci. Rep.* **2016**, 6, 32825.

[95] Axelrod, D.; Koppel, D.; Schlessinger, J.; Elson, E.; Webb, W. Mobility measurement by analysis of fluorescence photobleaching recovery kinetics. *Biophys. J.* **1976**, 16 (9), 1055–1069.

[96] Allan, D. B.; Caswell, T.; Keim, N. C.; Van der Wel, C. M. trackpy: Trackpy v0.4.1, **2018**.

[97] Van der Wel, C. M. Lipid Mediated Colloidal Interactions. Casimir PhD Series, **2017**.

[98] Sarfati, R.; Bławzdziewicz, J.; Dufresne, E. R. Maximum likelihood estimations of force and mobility from single short Brownian trajectories. *Soft Matter* **2017**, 13 (11), 2174–2180.

[99] Foreman-Mackey, D.; Hogg, D. W.; Lang, D.; Goodman, J. emcee: The MCMC Hammer. *ArXiv e-prints* **2013**, 125, 306.

[100] Gopalakrishnan, G.; Rouiller, I.; Colman, D. R.; Lennox, R. B. Supported bilayers formed from different phospholipids on spherical silica substrates. *Langmuir* **2009**, 25 (10), 5455–5458.

[101] Rädler, J.; Strey, H.; Sackmann, E. Phenomenology and Kinetics of Lipid Bilayer Spreading on Hydrophilic Surfaces. *Langmuir* **1995**, 11 (11), 4539–4548.

[102] Gözen, I.; Jesorka, A. Instrumental Methods to Characterize Molecular Phospholipid Films on Solid Supports. *Anal. Chem.* **2012**, 84 (2), 822–838.

[103] Macháň, R.; Hof, M. Lipid diffusion in planar membranes investigated by fluorescence correlation spectroscopy. *Biochim. Biophys. Acta* **2010**, 1798 (7), 1377–1391.

[104] Jing, Y.; Trefna, H.; Persson, M.; Kasemo, B.; Svedhem, S. Formation of supported lipid bilayers on silica: relation to lipid phase transition temperature and liposome size. *Soft Matter* **2014**, 10 (1), 187–95.

[105] Castillo, S. I. R.; Ouhajji, S.; Fokker, S.; Erné, B. H.; Schneijdenberg, C. T. W. M.; Thies-Weesie, D. M. E.; Philipse, A. P. Silica cubes with tunable coating thickness and porosity: From hematite filled silica boxes to hollow silica bubbles. *Microporous Mesoporous Mater.* **2014**, 195, 75–86.

[106] Cha, T.; Guo, A.; Zhu, X.-Y. Formation of Supported Phospholipid Bilayers on Molecular Surfaces: Role of Surface Charge Density and Electrostatic Interaction. *Biophys. J.* **2006**, 90 (4), 1270–1274.

[107] De Gennes, P. G. Polymers at an interface; a simplified view. *Adv. Colloid Interface Sci.* **1987**, 27 (3-4), 189–209.

[108] Upadhyayula, S.; Quinata, T.; Bishop, S.; Gupta, S.; Johnson, N. R.; Bahmani, B.; Bozhilov, K.; Stubbs, J.; Jreij, P.; Nallagatla, P.; Vullev, V. I. Coatings of polyethylene glycol for suppressing adhesion between solid microspheres and flat surfaces. *Langmuir* **2012**, 28 (11), 5059–69.

[109] Van der Wel, C.; Bossert, N.; Mank, Q. J.; Winter, M. G.; Heinrich, D.; Kraft, D. J. Surfactant-free colloidal particles with specific binding affinity. *Langmuir* **2017**, 33 (38), 9803–9810.

[110] Van Der Wel, C.; Van De Stolpe, G. L.; Verweij, R. W.; Kraft, D. J. Micrometer-sized TPM emulsion droplets with surface-mobile binding groups. *J. Phys.: Condensed Matter* **2018**, 30 (9).

[111] Naumann, C. A.; Prucker, O.; Lehmann, T.; Rühe, J.; Knoll, W.; Frank, C. W. The polymer-supported phospholipid bilayer: Tethering as a new approach to substrate-membrane stabilization. *Biomacromolecules* **2002**, 3 (1), 27–35.

[112] Tanaka, M.; Sackmann, E. Polymer-supported membranes as models of the cell surface. *Nature* **2005**, 437 (7059), 656–663.

[113] Tanaka, M. Polymer-Supported Membranes: Physical Models of Cell Surfaces. *MRS Bulletin* **2006**, 31, 513–520.

[114] Wagner, M. L.; Tamm, L. K. Tethered Polymer-Supported Planar Lipid Bilayers for Reconstitution of Integral Membrane Proteins: Silane-Polyethyleneglycol-Lipid as a Cushion and Covalent Linker. *Biophys. J.* **2000**, 79 (3), 1400–1414.

[115] Deverall, M. A.; Garg, S.; Ludtke, K.; Jordan, R.; Ruhe, J.; Naumann, C. A. Transbilayer coupling of obstructed lipid diffusion in polymer-tethered phospholipid bilayers. *Soft Matter* **2008**, 4, 1899–1908.

[116] Lipowsky, R. Bending of membranes by anchored polymers. *Europhys. Lett.* **1995**, 30 (4), 197.

[117] Geerts, N.; Eiser, E. DNA-functionalized colloids: Physical properties and applications. *Soft Matter* **2010**, 6 (19), 4647–4660.

[118] Valignat, M.-P.; Theodoly, O.; Crocker, J. C.; Russel, W. B.; Chaikin, P. M. Reversible self-assembly and directed assembly of DNA-linked micrometer-sized colloids. *Proc. Natl. Acad. Sci. U.S.A.* **2005**, 102 (12), 4225–4229.

[119] Biancaniello, P. L.; Crocker, J. C.; Hammer, D. A.; Milam, V. T. DNA-mediated phase behavior of microsphere suspensions. *Langmuir* **2007**, 23 (5), 2688–2693.

[120] Nordlund, G.; Lönneborg, R.; Brzezinski, P. Formation of Supported Lipid Bilayers on Silica Particles Studied Using Flow Cytometry. *Langmuir* **2009**, 25 (8), 4601–4606.

[121] Tan, A.; Ziegler, A.; Steinbauer, B.; Seelig, J. Thermodynamics of sodium dodecyl sulfate partitioning into lipid membranes. *Biophys. J.* **2002**, 83 (3), 1547–1556.

[122] Drobek, T.; Spencer, N. D.; Heuberger, M. Compressing PEG brushes. *Macromolecules* **2005**, 38 (12), 5254–5259.

[123] Meng, F.; Engbers, G. H. M.; Feijen, J. Polyethylene glycol-grafted polystyrene particles. *J. Biomed. Mater. Res. Part A* **2004**, 70 (1), 49–58.

[124] Garbuzenko, O.; Barenholz, Y.; Priev, A. Effect of grafted PEG on liposome size and on compressibility and packing of lipid bilayer. *Chem. Phys. Lipids* **2005**, 135 (2), 117–129.

[125] Angioletti-Uberti, S.; Varilly, P.; Mognetti, B. M.; Frenkel, D. Mobile linkers on DNA-coated colloids: Valency without patches. *Phys. Rev. Lett.* **2014**, 113 (12), 128303.

[126] Lipowsky, R. Spontaneous tubulation of membranes and vesicles reveals membrane tension generated by spontaneous curvature. *Faraday Discuss.* **2013**, 161, 305–331.

[127] Nakano, S. I.; Fujimoto, M.; Hara, H.; Sugimoto, N. Nucleic acid duplex stability: Influence of base composition on cation effects. *Nucleic Acids Res.* **1999**, 27 (14), 2957–2965.

[128] McMahon, H. T.; Gallop, J. L. Membrane curvature and mechanisms of dynamic cell membrane remodelling. *Nature* **2005**, 438 (7068), 590–596.

[129] Ewers, H.; Römer, W.; Smith, A. E.; Bacia, K.; Dmitrieff, S.; Chai, W.; Mancini, R.; Kartenbeck, J.; Chambon, V.; Berland, L.; et al. GM1 structure determines SV40-induced membrane invagination and infection. *Nat. Cell Biol.* **2010**, 12 (1), 11.

[130] Ehrlich, M.; Boll, W.; Van Oijen, A.; Hariharan, R.; Chandran, K.; Nibert, M. L.; Kirchhausen, T. Endocytosis by random initiation and stabilization of clathrin-coated pits. *Cell* **2004**, 118 (5), 591–605.

[131] Hess, S. T.; Gudheti, M. V.; Mlodzianoski, M.; Baumgart, T. Shape analysis of giant vesicles with fluid phase coexistence by laser scanning microscopy to determine curvature, bending elasticity, and line tension. In Methods in membrane lipids, 367–387. Springer, **2007**.

[132] Meijer, J.-m. Colloidal Crystals of Spheres and Cubes in Real and Reciprocal Space. *Springer theses* **2015**.

[133] Kim, J.-W.; Larsen, R. J.; Weitz, D. A. Synthesis of nonspherical colloidal particles with anisotropic properties. *J. Am. Chem. Soc.* **2006**, 128 (44), 14374–14377.

[134] Wang, Y.; Su, X.; Ding, P.; Lu, S.; Yu, H. Shape-controlled synthesis of hollow silica colloids. *Langmuir* **2013**, 29 (37), 11575–11581.

[135] Petruzielo, R. S.; Heberle, F. A.; Drazba, P.; Katsaras, J.; Feigenson, G. W. Phase behavior and domain size in sphingomyelin-containing lipid bilayers. *Biochim. Biophys. Acta, Biomembr.* **2013**, 1828 (4), 1302–1313.

[136] *https://github.com/RinaldinMelissa/SLVsAreaFraction* **2017**.

[137] Sezgin, E.; Levental, I.; Grzybek, M.; Schwarzmann, G.; Mueller, V.; Honigmann, A.; Belov, V. N.; Eggeling, C.; Coskun, Ü.; Simons, K.; et al. Partitioning, diffusion, and ligand binding of raft lipid analogs in model and cellular plasma membranes. *Biochim. Biophys. Acta* **2012**, 1818 (7), 1777–1784.

[138] Mukherjee, S.; Maxfield, F. R. Membrane domains. *Annu. Rev. Cell Dev. Biol.* **2004**, 20, 839–866.

[139] Ayuyan, A. G.; Cohen, F. S. Raft composition at physiological temperature and pH in the absence of detergents. *Biophys. J* . **2008**, 94 (7), 2654–2666.

[140] De Almeida, R. F.; Fedorov, A.; Prieto, M. Sphingomyelin/phosphatidylcholine/cholesterol phase diagram: boundaries and composition of lipid rafts. *Biophys. J.* **2003**, 85 (4), 2406–2416.

[141] Baumgart, T.; Hunt, G.; Farkas, E. R.; Webb, W. W.; Feigenson, G. W. Fluorescence probe partitioning between L o/L d phases in lipid membranes. *Biochim. Biophys. Acta, Biomembr.* **2007**, 1768 (9), 2182–2194.

[142] Provatas, N.; Elder, K. Phase-field methods in materials science and engineering. John Wiley & Sons, **2011**.

[143] Elliott, C. M.; Stinner, B. A surface phase field model for two-phase biological membranes. *SIAM J. Appl. Math.* **2010**, 70 (8), 2904–2928.

[144] Capovilla, R.; Guven, J. Stresses in lipid membranes. *J. Ph. A* **2002**, 35 (30), 302.

[145] Franzmann, T. M.; Jahnel, M.; Pozniakovsky, A.; Mahamid, J.; Holehouse, A. S.; Nüske, E.; Richter, D.; Baumeister, W.; Grill, S. W.; Pappu, R. V.; et al. Phase separation of a yeast prion protein promotes cellular fitness. *Science* **2018**, 359 (6371), eaao5654.

[146] Pontani, L.-L.; Haase, M. F.; Raczkowska, I.; Brujic, J. Immiscible lipids control the morphology of patchy emulsions. *Soft Matter* **2013**, 9 (29), 7150–7157.

[147] Hong-wei Wu, S.; McConnell, H. M. Phase separations in phospholipd membranes. *Biochemistry* **1975**, 14 (4), 847–54.

[148] Gebhardt, C.; Gruler, H.; Sackmann, E. On domain structure and local curvature in lipid bilayers and biological membranes. *Z. Naturforsch. C* **1977**, 32 (7-8), 581–96.

[149] Benvegnu, D. J.; McConnell, H. M. Line tension between liquid domains in lipid monolayers. *J. Phys. Chem.* **1992**, 96 (16), 6820–6824.

[150] Singer, S. J.; Nicolson, G. L. The fluid mosaic model of the structure of cell membranes. *Science* **1972**, 175 (4023), 720–31.

[151] Grayson, M. A. Shortening Embedded Curves. *Ann. Math.* **1989**, 129 (1), 71–111.

[152] Veatch, S. L.; Keller, S. L. Seeing spots: Complex phase behavior in simple membranes. *Biochimi. Biophys. Acta* **2005**, 1746 (3), 172–185.

[153] Brügger, B.; Sandhoff, R.; Wegehingel, S.; Gorgas, K.; Malsam, J.; Helms, J. B.; Lehmann, W.-D.; Nickel, W.; Wieland, F. T. Evidence for segregation of sphingomyelin and cholesterol during formation of COPI-coated vesicles. *J. Cell Biol.* **2000**, 151 (3), 507–518.

[154] Klemm, R. W.; Ejsing, C. S.; Surma, M. A.; Kaiser, H.-J.; Gerl, M. J.; Sampaio, J. L.; de Robillard, Q.; Ferguson, C.; Proszynski, T. J.; Shevchenko, A.; et al. Segregation of sphingolipids and sterols during formation of secretory vesicles at the trans-Golgi network. *J. Cell Biol.* **2009**, 185 (4), 601–612.

[155] Mouritsen, O. G.; Bagatolli, L. A. Life-as a matter of fat: lipids in a membrane biophysics perspective. Springer, **2015**.

[156] Markin, V. Lateral organization of membranes and cell shapes. *Biophys. J.* **1981**, 36 (1), 1–19.

[157] Taniguchi, T. Shape Deformation and Phase Separation Dynamics of Two-Component Vesicles. *Phys. Rev. Lett.* **1996**, 76 (23), 4444–4447.

[158] Jiang, Y.; Lookman, T.; Saxena, A. Phase separation and shape deformation of two-phase membranes. *Phys. Rev. E* **2000**, 61 (1), R57–R60.

[159] Góźdź, W. T. The interface width of separated two-component lipid membranes. *J. Phys. Chem. B* **2006**.

[160] Singh, P.; Mahata, P.; Baumgart, T.; Das, S. L. Curvature sorting of proteins on a cylindrical lipid membrane tether connected to a reservoir. *Phys. Rev. E* **2012**, 85 (5), 051906.

[161] Zhu, C.; Das, S. L.; Baumgart, T. Nonlinear Sorting, Curvature Generation, and Crowding of Endophilin N-BAR on Tubular Membranes. *Biophys. J.* **2012**, 102 (8), 1837–1845.

[162] Schick, M. Membrane heterogeneity: Manifestation of a curvature-induced microemulsion. *Phys. Rev. E* **2012**, 85 (3), 031902.

[163] Rautu, S. A.; Rowlands, G.; Turner, M. S. Membrane composition variation and underdamped mechanics near transmembrane proteins and coats. *Phys. Rev. Lett.* **2015**.

[164] McWhirter, J. L.; Ayton, G.; Voth, G. A. Coupling Field Theory with Mesoscopic Dynamical Simulations of Multicomponent Lipid Bilayers. *Biophys. J.* **2004**, 87 (5), 3242–3263.

[165] Baumgart, T.; Capraro, B. R.; Zhu, C.; Das, S. L. Thermodynamics and Mechanics of Membrane Curvature Generation and Sensing by Proteins and Lipids. *Annu. Rev. Phys. Chem.* **2011**, 62 (1), 483–506.

[166] Góźdź, W. T.; Bobrovska, N.; Ciach, A. Separation of components in lipid membranes induced by shape transformation. *J. Chem. Phys.* **2012**, 137 (1), 015101.

[167] Novick-Cohen, A.; Pego, R. L. Stable patterns in a viscous diffusion equation. *T. Am. Math. Soc.* **1991**, 324 (1), 331–351.

[168] Rubinstein, J.; Sternberg, P. Nonlocal reaction-diffusion equations and nucleation. *IMA J. Appl. Math.* **1992**, 48 (3), 249–264.

[169] Gómez, L. R.; García, N. a.; Vitelli, V.; Lorenzana, J.; Vega, D. a. Phase nucleation in curved space. *Nat. Commun.* **2015**, 6, 6856.

[170] Paillusson, F.; Pennington, M. R.; Kusumaatmaja, H. Phase Separation on Bicontinuous Cubic Membranes: Symmetry Breaking, Reentrant, and Domain Faceting. *Phys. Rev. Lett.* **2016**, 117 (5).

[171] Adkins, M. R.; Zhou, Y. Geodesic curvature driven surface microdomain formation. *J. Comput. Phys* **2017**, 345, 260–274.

[172] Jiang, H.; Powers, T. R. Curvature-Driven Lipid Sorting in a Membrane Tubule. *Phys. Rev. Lett.* **2008**, 101 (1), 018103.

[173] Wang, X.; Du, Q. Modelling and simulations of multi-component lipid membranes and open membranes via diffuse interface approaches. *J. Math. Biol* **2008**.

[174] Lowengrub, J. S.; Rätz, A.; Voigt, A. Phase-field modeling of the dynamics of multicomponent vesicles: Spinodal decomposition, coarsening, budding, and fission. *Phys. Rev. E* **2009**, 79 (3), 031926.

[175] Elliott, C. M.; Stinner, B. A Surface Phase Field Model for Two-Phase Biological Membranes. *SIAM Journal on Applied Mathematics* **2010**, 70 (8), 2904–2928.

[176] Jiang, H. Dynamic Sorting of Lipids and Proteins in Multicomponent Membranes. *Phys. Rev. Lett.* **2012**, 109 (19), 198101.

[177] Choksi, R.; Morandotti, M.; Veneroni, M. Global minimizers for axisymmetric multiphase membranes. *ESAIM Contr. Optim. Ca.* **2013**, 19 (4), 1014–1029.

[178] Helmers, M. Kinks in two-phase lipid bilayer membranes. *Calc. Var. Partial Differential Equations* **2013**.

[179] Hausser, F.; Marth, W.; Li, S.; Lowengrub, J.; Rätz, A.; Voigt, A. Thermodynamically consistent models for two-component vesicles. *Int. J. Biomath.* **2013**.

[180] Nelson, D.; Piran, T.; Weinberg, S. Statistical mechanics of membranes and surfaces. World Scientific, **2004**.

[181] Lázaro, G. R.; Pagonabarraga, I.; Hernández-Machado, A. Phase-field theories for mathematical modeling of biological membranes. *Chem. Phys. Lipids* **2015**, 185, 46–60.

[182] Crank, J. The mathematics of diffusion. Oxford University Press, **1979**.

[183] Schönborn, O.; Desai, R. C. Phase-ordering kinetics on curved surfaces. *Physica A* **1997**, 239 (1-3), 412–419.

[184] Goetz, R.; Helfrich, W. The Egg Carton: Theory of a Periodic Superstructure of Some Lipid Membranes. *J. Phys. II* **1996**, 6 (2), 215–223.

[185] Fournier, J. B.; Galatola, P. Tubular vesicles and effective fourth-order membrane elastic theories. *EPL* **1997**, 39 (2), 225–230.

[186] Siegel, D. P. Fourth-Order Curvature Energy Model for the Stability of Bicontinuous Inverted Cubic Phases in Amphiphile–Water Systems. *Langmuir* **2010**, 26 (11), 8673–8683.

[187] Deserno, M. Fluid lipid membranes: From differential geometry to curvature stresses. *Chem. Phys. Lipids* **2015**, 185, 11–45.

[188] Tolman, R. C. The Effect of Droplet Size on Surface Tension. *J. Chem. Phys.* **1949**, 17 (3), 333–337.

[189] Parisi, G. Statistical Field Theory. Frontiers in Physics. Addison-Wesley, **1988**.

[190] Geuzaine, C.; Remacle, J.-F. Gmsh: A 3D finite element mesh generator with built-in pre-and post-processing facilities. *Int. J. Numer. Meth. Eng.* **2009**, 79 (11), 1309–1331.

[191] Deuling, H.; Helfrich, W. The curvature elasticity of fluid membranes : A catalogue of vesicle shapes. *J. Ph.* **1976**, 37 (11), 1335–1345.

[192] Jenkins, J. T. Static equilibrium configurations of a model red blood cell. *J. Math. Biol.* **1977**, 4 (2), 149–169.

[193] Jülicher, F.; Lipowsky, R. Shape transformations of vesicles with intramembrane domains. *Phys. Rev. E* **1996**, 53 (3), 2670–2683.

[194] Sugimoto, T.; Khan, M. M.; Muramatsu, A.; Itoh, H. Formation mechanism of monodisperse peanut-type α-Fe_2O_3 particles from condensed ferric hydroxide gel. *Colloids Surf. A* **1993**, 79 (2-3), 233–247.

[195] Goodchild, J. A.; Walsh, D. L.; Connell, S. D. Substrate Roughness Significantly Affects Bilayer Phase Separation. *arXiv preprint arXiv:1902.01798* **2019**.

[196] Pathak, P.; London, E. Measurement of lipid nanodomain (raft) formation and size in sphingomyelin/POPC/cholesterol vesicles shows TX-100 and transmembrane helices increase domain size by coalescing preexisting nanodomains but do not induce domain formation. *Biophys. J.* **2011**, 101 (10), 2417–2425.

[197] McMahon, H. T.; Boucrot, E. Membrane curvature at a glance. *J. Cell Sci.* **2015**, 128 (6), 1065–1070.

[198] Knorr, R. L.; Staykova, M.; Gracià, R. S.; Dimova, R. Wrinkling and electroporation of giant vesicles in the gel phase. *Soft Matter* **2010**, 6 (9), 1990–1996.

[199] Staykova, M.; Arroyo, M.; Rahimi, M.; Stone, H. A. Confined bilayers passively regulate shape and stress. *Phys. Rev. Lett.* **2013**, 110 (2), 028101.

[200] Mim, C.; Unger, V. M. Membrane curvature and its generation by BAR proteins. *Trends Biochem. Sci.* **2012**, 37 (12), 526–533.

[201] Keber, F. C.; Loiseau, E.; Sanchez, T.; DeCamp, S. J.; Giomi, L.; Bowick, M. J.; Marchetti, M. C.; Dogic, Z.; Bausch, A. R. Topology and dynamics of active nematic vesicles. *Science* **2014**, 345 (6201), 1135–1139.

[202] Oláh, A.; Hillborg, H.; Vancso, G. J. Hydrophobic recovery of UV/ozone treated poly (dimethylsiloxane): adhesion studies by contact mechanics and mechanism of surface modification. *Appl. Surf. Sci.* **2005**, 239 (3-4), 410–423.

[203] Brewer, L. R.; Bianco, P. R. Laminar flow cells for single-molecule studies of DNA-protein interactions. *Nat. Methods* **2008**, 5 (6), 517.

[204] Reits, E. A.; Neefjes, J. J. From fixed to FRAP: measuring protein mobility and activity in living cells. *Nat. Cell Biol.* **2001**, 3 (6), E145.

[205] Lippincott-Schwartz, J.; Snapp, E.; Kenworthy, A. Studying protein dynamics in living cells. *Nat. Rev. Mol. Cell Biol.* **2001**, 2 (6), 444.

[206] Haas, K.-H.; Wolter, H. Synthesis, properties and applications of inorganic–organic copolymers (ORMOCER® s). *Curr. Opin. Solid State Mater. Sci.* **1999**, 4 (6), 571–580.

[207] Schlie, S.; Ngezahayo, A.; Ovsianikov, A.; Fabian, T.; Kolb, H.-A.; Haferkamp, H.; Chichkov, B. N. Three-dimensional cell growth on structures fabricated from ORMOCER® by two-photon polymerization technique. *J. Biomater. Appl.* **2007**, 22 (3), 275–287.

[208] Renner, M.; Domanov, Y.; Sandrin, F.; Izeddin, I.; Bassereau, P.; Triller, A. Lateral diffusion on tubular membranes: quantification of measurements bias. *PLoS One* **2011**, 6 (9), e25731.

[209] Brünger, A.; Peters, R.; Schulten, K. Continuous fluorescence microphotolysis to observe lateral diffusion in membranes. Theoretical methods and applications. *J. Chem. Phys.* **1985**, 82 (4), 2147–2160.

[210] Aizenbud, B. M.; Gershon, N. D. Diffusion of molecules on biological membranes of nonplanar form. A theoretical study. *Biophys. J.* **1982**, 38 (3), 287–293.

[211] Sbalzarini, I. F.; Hayer, A.; Helenius, A.; Koumoutsakos, P. Simulations of (an) isotropic diffusion on curved biological surfaces. *Biophys. J.* **2006**, 90 (3), 878–885.

[212] Wang, M.; Liu, Z.; Zhan, W. Janus Liposomes: Gel-Assisted Formation and Bioaffinity-Directed Clustering. *Langmuir* **2018**, 34 (25), 7509–7518.

[213] Langecker, M.; Arnaut, V.; List, J.; Simmel, F. C. DNA nanostructures interacting with lipid bilayer membranes. *Acc. Chem. Res.* **2014**, 47 (6), 1807–1815.

[214] Czogalla, A.; Petrov, E. P.; Kauert, D. J.; Uzunova, V.; Zhang, Y.; Seidel, R.; Schwille, P. Switchable domain partitioning and diffusion of DNA origami rods on membranes. *Faraday Discuss.* **2013**, 161, 31–43.

[215] Czogalla, A.; Franquelim, H. G.; Schwille, P. DNA nanostructures on membranes as tools for synthetic biology. *Biophys. J.* **2016**, 110 (8), 1698–1707.

[216] Kato, A.; Tsuji, A.; Yanagisawa, M.; Saeki, D.; Juni, K.; Morimoto, Y.; Yoshikawa, K. Phase separation on a phospholipid membrane inducing a characteristic localization of DNA accompanied by its structural transition. *J. Phys. Chem. Lett* **2010**, 1 (23), 3391–3395.

[217] Cademartiri, L.; Bishop, K. J. Programmable self-assembly. *Nature Mat.* **2014**, 14 (1), 2.

[218] Bunge, A.; Kurz, A.; Windeck, A.-K.; Korte, T.; Flasche, W.; Liebscher, J.; Herrmann, A.; Huster, D. Lipophilic oligonucleotides spontaneously insert into lipid membranes, bind complementary DNA strands, and sequester into lipid-disordered domains. *Langmuir* **2007**, 23 (8), 4455–4464.

[219] Kurz, A.; Bunge, A.; Windeck, A.-K.; Rost, M.; Flasche, W.; Arbuzova, A.; Strohbach, D.; Müller, S.; Liebscher, J.; Huster, D.; et al. Lipid-anchored oligonucleotides for stable double-helix formation in distinct membrane domains. *Angew. Chem. Int. Ed.* **2006**, 45 (27), 4440–4444.

[220] Klassische Runge-Kutta-Formeln vierter und niedrigerer Ordnung mit Schrittweiten-Kontrolle und ihre Anwendung auf Wärmeleitungsprobleme. *Comput.* **1970**, 6 (1-2), 61–71.